Assessing daylight performance in use

A comparison between long-term daylight measurements and simulations

Brembilla, E.; Drosou, N. C.; Mardaljevic, J.

DOI
10.1016/j.enbuild.2022.111989

Publication date
2022

Document Version
Final published version

Published in
Energy and Buildings

Energy & Buildings 262 (2022) 111989

Contents lists available at ScienceDirect

Energy & Buildings

journal homepage: www.elsevier.com/locate/enb

Assessing daylight performance in use: A comparison between long-term daylight measurements and simulations

E. Brembilla [a,*], N.C. Drosou [b], J. Mardaljevic [b]

[a] Department of Architectural Engineering and Technology, Delft University of Technology, Delft, The Netherlands
[b] School of Architecture, Building and Civil Engineering, Loughborough University, Loughborough, UK

ARTICLE INFO

Article history:
Received 30 November 2021
Revised 21 February 2022
Accepted 24 February 2022
Available online 4 March 2022

Keywords:
Climate-based daylight modelling (CBDM)
High dynamic range imaging (HDRI)
Long-term monitoring
Operational performance

ABSTRACT

Climate-Based Daylight Modelling (CBDM) methods have been validated against long-term measurements in laboratory settings and found to exhibit errors small enough to make such assessments useful for daylight performance prediction. However, real occupied spaces are affected by a higher number of uncertainties than laboratory or controlled conditions. This study aims at validating CBDM methods against measurements collected in an occupied classroom space, where a monitoring system based on High Dynamic Range Imaging was installed. Four vertical regions were identified on two of the room's walls, and mean illuminance was calculated for these regions at every time step, both from HDR images and from simulated results. Two simulation methods were evaluated: the 2-phase and the 4-component methods. Sun and sky conditions for the simulations were derived from simultaneous monitored irradiation measurements. Both simulation methods led to moderate over-prediction of HDR-derived results, when considering instantaneous illuminance means and when looking at long-term metrics (cumulative irradiation and Useful Daylight Illuminance). Wall regions exposed to more direct sky- and sunlight were characterised by smaller systematic errors (rMBE = 4%) but similar variance (r^2 = 0.83) than regions situated at the back of the room (rMBE = 17–34% and rMAE = 27–37%). Further studies are needed to identify and separate the sources of such errors.

1. Introduction

Building performance simulation is a powerful tool for assessing design options and their relative environmental performance. Assessments performed at the design stage often contain numerous assumptions regarding the form and composition of the building since many details are yet unknown to designers and engineers. At the operational stage, the behaviour of actual occupants is likely to further increase the uncertainty of building performance predictions. Occupants might modify the internal layout (e.g., adding furniture and decorations) or interact with building systems in unexpected ways (e.g., keeping blinds down more often than required and using electric lighting instead). It is therefore expected that initial performance results will differ from the actual performance of a building in use. However, it is very important to understand where the causes of this discrepancy might lie and try to improve initial prediction models accordingly.

A vast literature explored the subject of the "performance gap" in energy simulation [1–4] since this issue was first brought up [5]. There is however still much research to be done on the "daylight performance gap", especially in relation to annual performance and evaluation in occupied spaces under normal usage.

Daylighting practice went through a fundamental transition when Climate-Based Daylight Modelling (CBDM) was introduced in the late 1990s [6,7]. Rather than limiting the assessments to standard sky models (typically overcast and clear), CBDM includes a range of intermediate sky conditions and, using sky models, characterises them based on irradiance and illuminance values found in weather files. This makes it possible to assess long-term daylight conditions and facilitates the integration with other building performance analyses, e.g., energy or thermal comfort, which are based on the same weather data. Moreover, dealing with absolute simulation results allows model validation and calibration against field measurements. On the other hand, absolute values require higher accuracy in input data and taking into account their uncertainties become even more relevant. For validation of CBDM metrics, it is also necessary to run measurement or monitoring campaigns over long periods of time, in order to capture the variability of daylight conditions over different seasons. Validations

* Corresponding author at: Department of Architectural Engineering and Technology, Faculty of Architecture, Building 8, Julianalaan 134, Delft University of Technology, 2628 BL Delft, The Netherlands.
E-mail address: E.Brembilla@tudelft.nl (E. Brembilla).

https://doi.org/10.1016/j.enbuild.2022.111989
0378-7788/

performed in laboratory settings [8,9] characterised errors typical for daylight 'matrix methods' (or 'phase methods') as being within ±20%. Among Post-Occupancy Evaluation (POE) studies that focused on the validation of daylight and visual comfort metrics against subjective occupant impressions in existing buildings, only very few looked at long-term daylight performance [10,11]. The study performed by Jakubiec, Quek, and Srisamranrungruang [11] is the most comprehensive to date, but measurements were only collected once and used to calibrate the simulation models [12], whose results were then correlated to subjective responses of visual comfort.

The successful integration of daylight with artificial lighting at the design stage requires confidence in the reliability of simulated climate-based measures of daylight [13,14]. In 2013, the UK Education Funding Agency (EFA) made climate-based daylight modelling a mandatory requirement for the evaluation of designs submitted for school building programmes. This was the first major upgrade to mandatory daylight requirements since the introduction of the daylight factor more than half a century ago. Unsurprisingly, this decision was seen as controversial by some practitioners/researchers, in part because it was claimed that CBDM metrics were difficult if not impossible to verify in actual buildings [15]. Whilst there was a sizeable body of evidence from validation studies indicating the likely potential reliability of the CBDM approach itself [16], the question regarding the in situ validation of CBDM metrics for actual occupied buildings remains.

The present study compares CBDM results with daylight measurements collected in a in-use classroom over a period of over 8 months. An unprecedented collection of 14670 High Dynamic Range (HDR) images allowed the measurement of indoor luminance at 10-minute resolution without disturbing occupants' activities. Compared to validations performed in test laboratories, which focus more on the *physical* validity of simulated output, this comparison aims at providing information with regard to modelling assumptions and uncertainties.

2. Methods

This study compares two datasets of long-term indoor illuminance values, obtained with two different methods: (1) by monitoring a real, in-use classroom via an HDRI system, and by using the luminance maps and known reflectance to derive illuminance; and (2) by simulating indoor illuminance using two CBDM methods, which relied on locally measured irradiance data to simulate sky conditions.

The space used for the study is one of the four classrooms selected for a wider research on daylight performance in schools [17]. These four classrooms, located in two different school buildings, were continuously monitored for a period of 8 to 12 months. The room used in the present paper is located in Loughborough, UK (geographical coordinates: 52.77 N; 1.2 W) and it is illustrated in Fig. 1. It is a side-lit space with a fully fenestrated facade, looking towards North-West (27°from due North). Shading devices were not installed during the monitoring period. At the time, the room was used for various educational activities, including face to face teaching classes and practical sessions.

2.1. HDRI-based monitoring

The room was monitored for a total of almost a year, starting from the 3rd April 2015 until 4th April 2016. A Canon EOS 600D Digital SLR camera, fitted with an ultra wide-angle Canon EF-S 10–18 mm lens and tethered to a MacMini computer for automatic capture and storage of images, comprised the self-contained capture equipment. This was placed in a corner of the classroom and oriented towards the interior space. The aperture was set to $f8$, the sensitivity to ISO 100 and the white balance to 'Daylight'. The focussing mode was set to manual and the focus checked/adjusted for sharpness once the camera was in position. The HDR capture sequence was controlled by a timed script which was executed every 10 min between 08:00 and 17:50 using the UNIX *cron* function. Each HDR capture comprised a sequence of seven ordinary low dynamic range (LDR) images taken in quick succession using a fixed aperture ($f8$) and varying shutter speed covering the range 1/2000 s to 2 s in two exposure stop increments, i.e. 1/2000, 1/500, 1/125 s, etc. Immediately following each capture, the seven LDR images were compiled into a HDR image using the hdrgen program with a predetermined HDR image response calibration file. Note, the response file was created from a scene including direct sun illumination on white painted surfaces and calibrated against luminance measurements taken with a Konica Minolta LS-100 luminance meter. To save disk storage space, the LDR images were deleted after the HDR image was generated. Each newly generated HDR image was then tested for mean scene luminance, and those registering zero or very low luminance levels (i.e. taken under largely dark conditions) were deleted to further save disk space. The remaining HDR image (already saved to the MacMini primary drive) was then uploaded to a cloud server.

2.2. Climate-based daylight modelling

Simulation results were obtained with two different CBDM methods: the two-phase method (2PH, also known as *daylight coefficient* method) and the four-component method (4CM) [6], which are respectively the more common and the more thoroughly validated methods to simulate clear glazing systems. Both are based on the *Radiance* ray-tracing engine [18] but they use two different approaches, based on the *rcontrib* and on the *rtrace* commands respectively. For the 2PH to produce more accurate results of direct sunlight, a sky discretization scheme with 5185 patches (MF:6) was used. The Radiance parameters set for the ambient calculation in the 2PH were: `-ab 5 -ad 100000 -lw 1e-5`. For the 4CM, which is based on the `rtrace` command and uses ambient interpolation[1], the parameters were: `-ad 4096 -ab 7 -ar 256 -as 256 -aa 0.2 -lw 0.001 -lr 10`. Furniture was not included in the virtual model. Reflectance properties of the interior surfaces were derived from combined measurement of luminance and illuminance, under the assumption that they exhibited Lambertian properties (i.e., perfectly diffusing surfaces). Glass transmittance was determined from manufacturer's specification sheets found for the installed window model and type (double-glazed insulated unit). These optical properties, reported in Table 1, were then assigned to the simulation model.

Virtual sensor points were placed in the *Radiance* model to represent the same four regions identified in the HDR images. Their position was specified in two different ways for the two simulation methods. For the 2PH, a coarse grid with a spacing of 0.50 m was created over the wall regions, for a total of 37 data points. For the 4CM, which applies ambient interpolation, it was possible to use a finer grid resolution, for a total of 1556 points. The difference between the number of points defined in the two methods is significant but not relevant here, as the scope of this work was not to compare their performance relative to each other but relative to the HDR measurements.

Both methods used the Perez All-Weather model [19] to derive the sky luminance distribution from irradiance data. Irradiance was measured at a weather station established 1.7 km away from the classroom. A Delta-T SPN1 pyranometer with fixed shading

[1] Note, unlike the various 'phased' *Radiance* CBDM approaches, the 4CM takes full advantage of both the keystone ambient interpolation algorithm and the overture calculation to significantly reduce random variance (i.e., 'lumpiness') in the results.

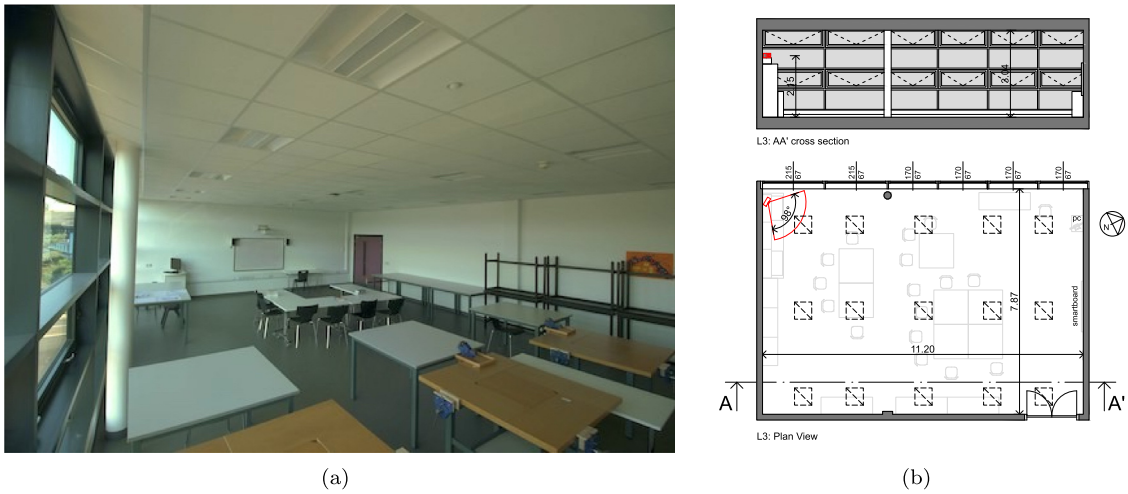

(a) (b)

Fig. 1. Classroom used as case study. (a) Interior view from the viewpoint of the HDR camera and (b) technical drawing showing the room in plan view and as a cross section. In the plan view the approximate position of furniture and the position of the ceiling-mounted lamps are indicated.

Table 1
Optical properties of the main geometrical elements found in the classroom and applied to the simulation model. Reflectances are based on measured values, whereas transmittance is based on manufacturer's specifications.

ρ Floor	ρ Walls	ρ Ceiling	ρ Window frames	ρ External surfaces	T_{vis} Window transmittance	Window transmissivity
0.25	0.90	0.85	0.10	0.30	0.68	0.74

mask measured global and diffuse horizontal irradiance time series, from which direct normal irradiance could also be derived [20]. Measurements were recorded at 1-minute resolution and later averaged over 10 minute time steps. As part of the quality control procedure, any global and diffuse value recorded while the sun was below the horizon, and any direct normal value recorded for sun altitudes lower than 1 degree, were considered to be equal to zero. A data loss in irradiance records meant that simulations could only be performed starting from 22-07-2015. Irradiance data from other sources (e.g., weather stations further away or satellite data) could be used to fill the gap in the irradiance time series, but that would introduce additional uncertainties and was therefore not considered for the present study.

2.3. Comparison between measurements and simulation

The comparison between measured and simulated results was based on vertical illuminance values. To derive illuminance from the luminance values obtained with HDRI, a method based on the Lambertian reflection equation was applied as described in more detail by [21]. Such method derives the illuminance field falling onto a surface from luminance maps, by applying the equation

$$E = \frac{L\pi}{\rho} \quad [\mathrm{lx}] \tag{1}$$

and by interpolating the resulting illuminance across multiple regions of known reflectance.

Four regions at the upper side of two walls (see Fig. 2) were identified as being free from obstructions for most of the monitoring period and therefore suitable to be characterised by a single constant reflectance value ($\rho_w = 0.90$ in this case). This choice also gave reasonable certainty that space occupants' presence and movements would be unlikely to significantly affect luminance values measured by the HDRI system. An additional region (named H1 in Fig. 2) was defined to compare HDR-derived illuminance values and measurements recorded by a wall-mounted Hanwell illuminance meter at 1-minute intervals (spectral response error 5%; linear response error 1%). The illuminance meter was placed away from possible exposure to direct sunlight, as that could have reached the measuring upper limit of the sensor (5000 lx). The meter was installed in the classroom from 17-11-2015 to 28-03-2016. These data were used for a preliminary validation of the HDR-derived illuminance measurements. They were also used as a control for potential time drift effects in the HDR luminance series, which might appear if the shutter mechanism slows down due to mechanical fatigue.

When applied for building evaluation purposes, CBDM is generally used to assess long-term daylighting performance in terms of particular metrics. To investigate the long-term accuracy of the 4CM and 2PH against HDR measurements, two metrics were chosen: cumulative illumination, expressed in *klx hr*, and Useful Daylight Illuminance (UDI), expressed as a percentage of the analysed period. For UDI, four ranges were considered: 0-100 lx (UDI-n); 100-300 lx (UDI-s); 300-3000 lx (UDI-a); and over 3000 lx (UDI-e). In contrast to the more usual applications of UDI, here this metric is calculated from *vertical* illuminance values.

3. Results

The results extracted from the HDR monitoring dataset and those obtained from simulations are presented in this section. An overview of all the data measured and collected over the monitoring period is presented at first, in Section 3.1. Then Section 3.2 presents the first data comparison, between HDR-derived and measured illuminance, used as a control of the quality and consistency of the HDR images. Last, Section 3.3 looks at the comparison between HDR-derived and simulated illuminance.

3.1. Overview of the collected data

All measured quantities are first presented here, to show the range of values that characterised the recorded time series and

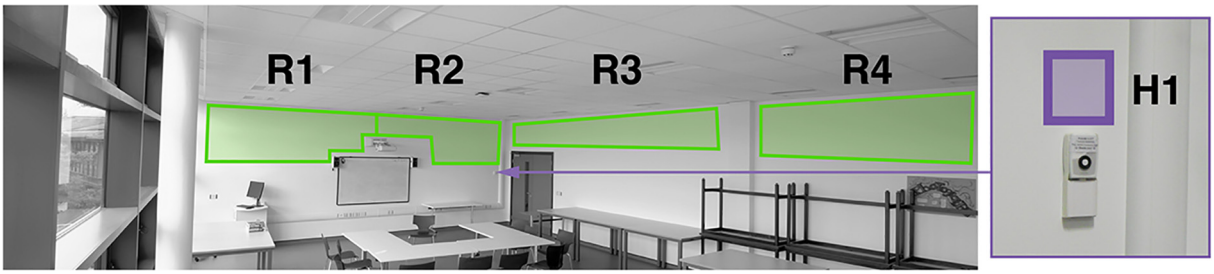

Fig. 2. Regions (R1 to R4) identified in the HDR images as having no or little obstructions throughout the analysis period. The same regions were defined when setting up analysis grids in the 2PH and 4CM simulations. Region H1, enlarged next to the main image, was used to compare HDR-derived illuminances with those measured by the luxmeter mounted just below.

to visualise side-by-side the periods in which measurements were collected. Fig. 3 shows the different types of data collected during the entire monitoring period. Fig. 3a shows the mean luminance recorded by HDR images over the four regions of interest (R1 to R4). Each point represents the mean luminance from a single region. From the HDR images, it was also possible to detect the instances in which the electric lighting system was switched on. The graph indicates those instances together with their relative HDR-derived illuminance in yellow colour. In the following analyses, only instances with all lights switched off were considered. Fig. 3b shows illuminance values measured by the wall-mounted illuminance meter. Fig. 3c shows the outdoor irradiance recorded by the local pyranometer, with both global and diffuse horizontal components (GHI and DHI).

The luminance data shown in Fig. 3a were then converted to illuminance values for the comparison with simulated results. The irradiance values shown in Figure 3c were used in the simulations as input to the Perez All-Weather sky model; direct normal irradiance was derived from GHI and DHI.

3.2. Validation of HDR-derived illuminance data

Fig. 4 shows the difference between illuminance derived from HDR images and illuminance measured by the illuminance meter, over the time period of its installation. Fig. 4a shows the correlation between the two datasets. The correlation is highly linear and the coefficient of determination r^2 is 0.96, indicating a very close agreement. In 4b, instantaneous differences are plotted over the considered time period. Peaks are noticeable throughout this period, but they can be reliably considered outliers, as most of them correspond to instances in which the classroom door was open and covered the illuminance meter. All such outliers fall outside the 'whiskers' of a boxplot distribution graph and constitute 1% of the dataset. Considering outliers, the Mean Bias Error (MBE) is +20 lx (rMBE = +10%) and the Root Mean Square Error (RMSE) is ±33 lx (rRMSE = ±16%). The errors do not exhibit any time-related trend and time drift effects can therefore be excluded. These results give confidence that the HDR-derived illuminance data are sufficiently reliable to serve as the datum for the comparison that follows.

3.3. Comparison between HDR-derived and simulated illuminance data

The core part of the analysis, presented in this section, takes the illuminance derived from the HDR images as a benchmark to assess the accuracy of simulation results in a real space. The analysis looks at the agreement between mean vertical illuminance obtained from HDR images and simulated using either the 2PH or the 4CM methods. Fig. 5 shows the error distribution histograms for the four regions illustrated above (see Fig. 2). Overall, the errors exhibited by the 2PH and the 4CM are similar, with the 4CM performing marginally better, especially when looking at the region closest to the window (R1). Such region is the one that receives most direct sunlight among the four analysed regions. Given the fact that the 4CM is based on a finer representation of the sun and uses a higher resolution analysis grid, its higher accuracy when compared to the 2PH was expected. For all other regions (R2–R4), the rMBE is within a 17–34% range and the relative Mean Absolute Error (rMAE) is within a 27–37% range. The boxplots placed above the histograms show that 50% of the error population (i.e., within the box limits) lies within a -30 to 168 lx range, whereas 96% of the errors (i.e., within the whiskers) lies within a -370 to 544 lx range.

To describe in more detail the errors that characterise the single instances in time, a scatterplot showing the relationship between the HDR-derived and the simulated illuminance datasets is presented in Fig. 6. It is evident that errors tend to increase for higher illuminance values. In the case of R1, also the scatter is more pronounced for high illuminance instances, corresponding to times when direct sunlight enters the room directly and falls in the analysed region. For all regions and for both simulation methods, the coefficient of determination r^2 is close or over 0.80, indicating a close relationship between the two datasets (measured and simulated). Such relationship is however not linear, as the variance increases for higher illuminance values.

Whilst the errors for the point-in-time instances are revealing, for practical application it is arguably the case that outcomes based on a comparison of CBDM metrics is just as important. Fig. 7 shows (a) the cumulative illumination, and (b) UDI values, calculated from vertical illuminances obtained from the three methods (HDR, 2PH and 4CM). The error bars reported in Fig. 7a represent a 12% error, corresponding to the rRMSE found in the analysis presented in Section 3.2. The over-prediction of simulated results that was observed in the previous analysis also affects long-term metrics. The difference in cumulative illumination as calculated with the 4CM and the 2PH, relative to HDR results, closely matches the statistical errors found for illuminance values. For R1, the 4CM over-predicts HDR-derived illuminance values by 5% and the 2PH by 19%; for the other regions, both method over-predict measured values by 17–34%. UDI results show the same trend, with lower illuminance ranges (UDI-n) being underpredicted by simulation methods. There were very few instances in which the vertical illumination exceeded 3000 lx, therefore the UDI-e range was equal to zero in all cases.

4. Discussion

Results presented in this paper show that simulated vertical illuminance values tend to over-predict illuminances derived from HDR images collected from the actual, in-use space. Systematic

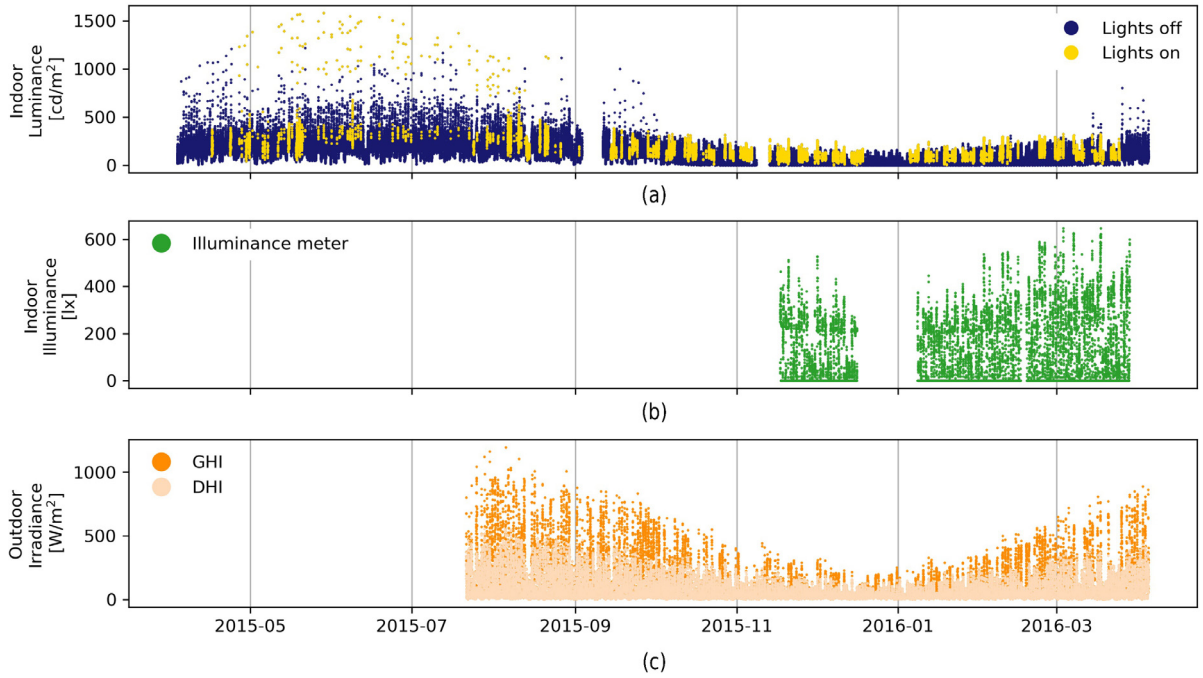

Fig. 3. Overview of the data collected during the study period. (a) Luminances measured by the HDR camera within each of the four wall regions; instances in which the electric lighting system was switched on are highlighted. (b) Illuminances measured by the wall-mounted lux meter. (c) Irradiance values (global and diffuse horizontal) locally measured by a pyranometer.

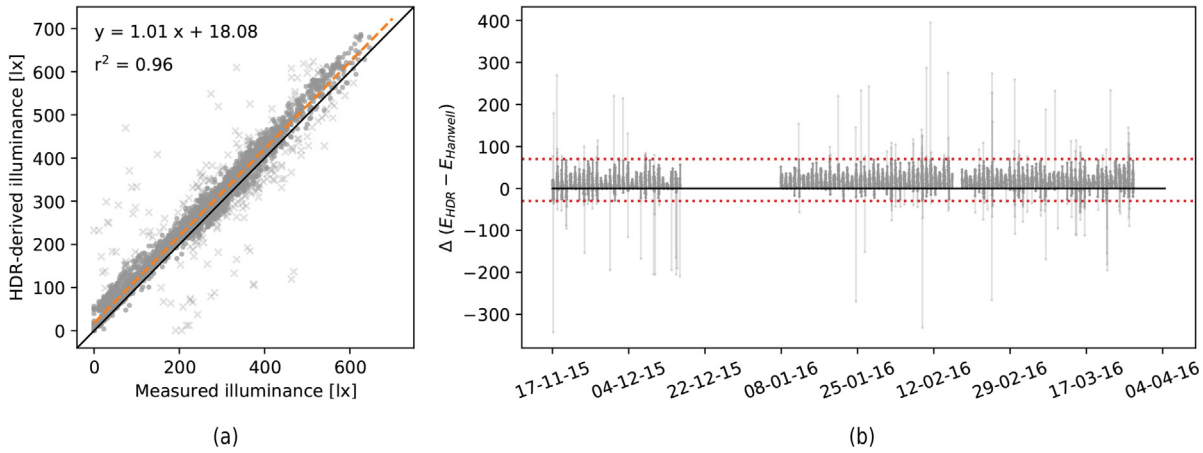

Fig. 4. Regression and error analysis for the illuminance derived from HDR images, compared to illuminance measured by the lux meter. (a) The regression line is shown in the scatterplot as an orange dashed line and its equation is indicated above. (b) The horizontal dashed lines indicate the limits beyond which data points were considered outliers (-30lx to 70lx).

errors (MBE) range between +4% and +34%, whereas random errors (MAE) vary between ±18% and ±37%. CBDM metrics, such as UDI, are affected by similar errors. As expected, these errors are larger than those found when validating simulation methods in laboratory setting (±20%). However, trends and correlations between simulated and HDR-derived display promising outcomes for a field study in an occupied building.

The higher systematic errors characterising the wall regions at the back of the room seem to suggest that the main source of error is in the simulation of predominantly reflected light, rather than with the prediction of the (sun and sky) direct contributions. The fact that furniture and other detailed elements were not included in the virtual model certainly contributes to the uncertainty related to light redistribution within the space. The general trend noticed in simulated results to over-predict HDR-derived illuminance might be related to these same factors, as the elements present in the actual room might block daylight redistribution and reduce illuminance levels on the walls. Trying to represent the actual furniture – which was constantly rearranged by the occupants – was impractical for this study. However, for future studies, automated object recognition algorithms could perhaps be used to identify the position of the elements in the room and modify the virtual model accordingly. Another cause for the over-estimation exhibited by simulation could be the specification of reflectance and transmittance values in the virtual model, factors that are known to affect final results [22]. Window transmittance is often further reduced by maintenance factors, not included in the present analysis, and has a direct effect on the amount of daylight entering a space. Such errors could be potentially reduced by model calibration.

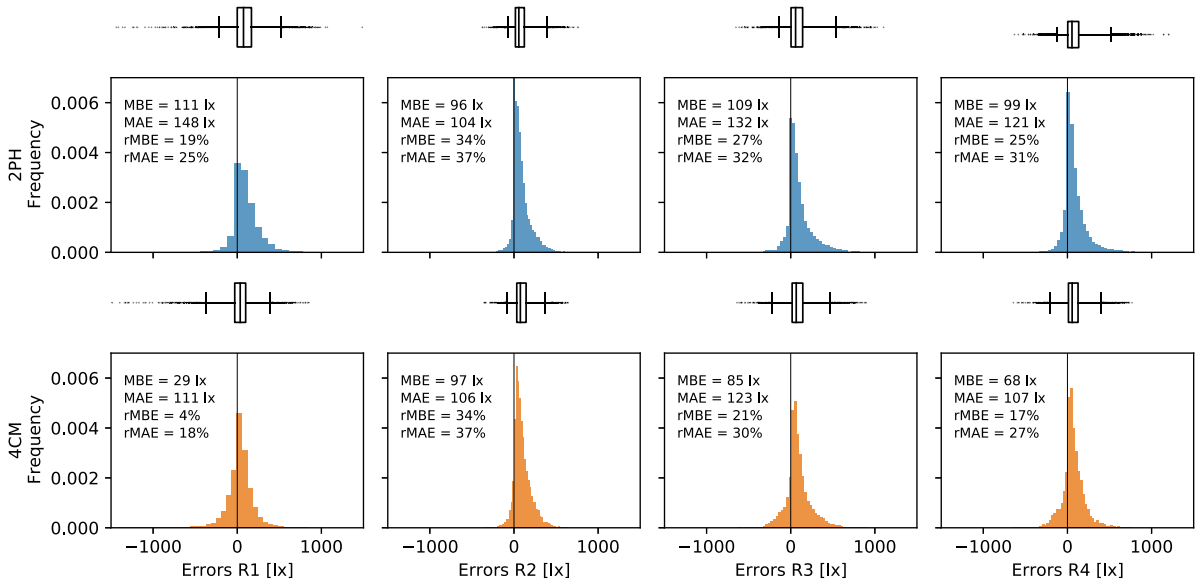

Fig. 5. Histograms of errors found for the 2PH (top row) and for the 4CM (bottom row), for the four wall regions. The histograms are accompanied by the absolute and relative values of mean bias and mean absolute errors. At the top of the histograms, a boxplot is also presented, to show more clearly the error distribution and the values that lie beyond the box whiskers (i.e., beyond the 2nd and 98th percentile limits).

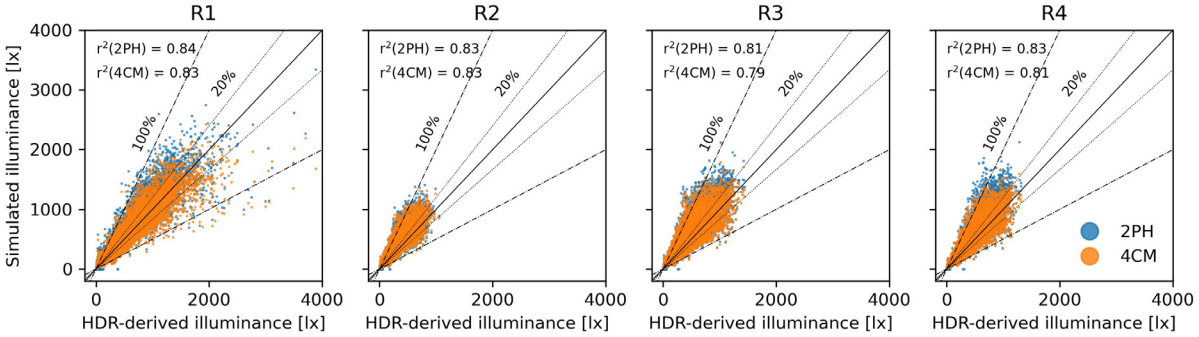

Fig. 6. Scatterplots showing the relation between HDR-derived and simulated illuminances, for both simulation methods 2PH and 4CM. Error intervals and coefficients of determination are also presented, for each of the four regions under analysis.

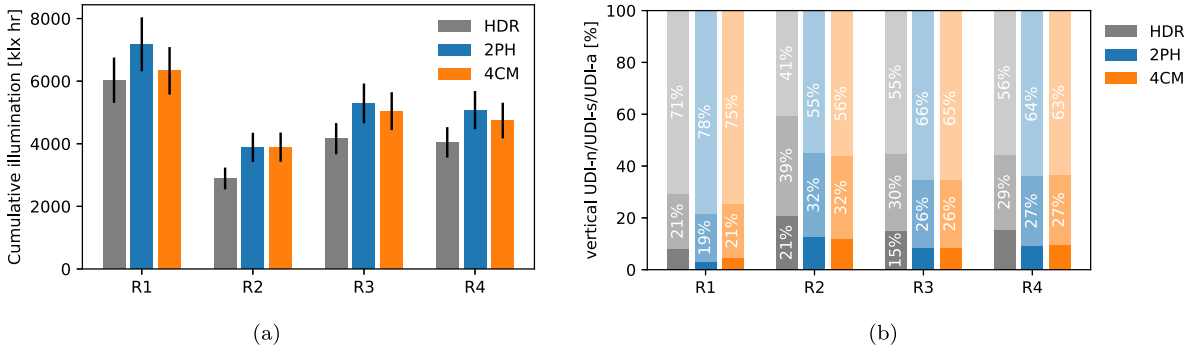

Fig. 7. (a) Mean cumulative illumination falling onto the four wall regions and (b) mean UDI ranges characterising the same regions. The UDI-e range (> 3000 lx) is not displayed as it was zero in all instances. Error bars indicate the error found when comparing HDR-derived and measured illuminances (12%).

When analysing the scatterplot showing HDR-derived against simulated illuminance (Fig. 6), variance was found to increase proportionally with illuminance values. This could be interpreted as an incremental effect of the errors due to aforementioned factors when outdoor illuminance levels are higher, i.e., for clear sky/-sunny conditions. On the other hand, the HDR-based procedure to derive illuminance could be also affected by higher errors for instances of high luminance, even though this effect is not displayed in the range 0–700 lx investigated in Section 3.2 or in previ-

ous studies carried out with the same setup [21]. Future research should further investigate and clarify this point.

Physical characterisation of the immediate external environment facing the windows of the classroom contains potentially significant uncertainties. In keeping with typical modelling practices, a generic ground reflectance value of 0.20 was used, and the ground geometry was modelled as a single polygon. The actual ground area outside the classroom comprises a mixture of car parking space (black tarmac), footpaths (also tarmac) and some planting area with foliage and trees. Taken together, it seems a reasonable proposition that the actual reflectance of the ground environment facing the classroom windows is lower than the canonical value of 0.20 commonly used in simulations. Accordingly, this could explain some or much of the noted tendency for over-prediction by both simulation methods.

Regions at the top of vertical walls were chosen for this analysis, as the method to derive illuminance values from HDR images requires areas that are less likely to be cluttered by other objects or be occasionally obstructed by occupants, i.e., areas whose reflectance properties can be assumed to be constant during the entire duration of the study. However, these regions are less likely to represent the general daylight performance of the space. For daylight sufficiency analyses, it is common to define an horizontal plane at desk height, and CBDM metrics are usually calculated from illuminance values simulated on such plane. Future work should look at whether the performance at desk level could be derived from data collected elsewhere in a room with a sufficient level of confidence. This could be used in further studies investigating the accuracy of CBDM metrics and advance our understanding of how they correlate with human's perception of daylight levels in indoor spaces.

The analysis was carried out with data from a single space, hence it is not sufficient to draw any generalised conclusion about the gap between simulated and actual daylight performance. However, it is reasonable to assume that simulating an empty space at design stage will lead to an over-prediction of the daylight performance characterising the same space once it is occupied and filled with furniture and appliances. Long-term data on daylight levels in occupied spaces would need to be collected to generalise the present findings, ideally from many different building types. Both indoor- and outdoor-mounted HDR-based monitoring systems for the control of shading devices are under development [23–25]. Data from this type of systems could be also used to assess and improve models currently implemented in daylight simulation. Furthermore, the light monitoring method used in this paper could offer a non-intrusive and data-rich solution to long-term POE studies on visual comfort.

5. Conclusion

To assess the daylight performance of a space, data about the daily and seasonal variability of daylight are required. CBDM methods allow the simulation of such variability through the use of representative weather data. To validate such methods, measurements should be collected in real spaces over long time periods (i.e., at least several months). This has been previously done for laboratory settings, where the daylight performance could be monitored under controlled conditions. However, the expected 'laboratory' accuracy might be severely affected by uncertainties characterising real spaces. This study aimed at validating CBDM methods and metrics against measurements collected in an occupied classroom space, with the help of an HDR-based monitoring system.

Vertical illuminance simulated with the 2PH and the 4CM methods was compared with illuminance values derived from HDR images, collected every 10 min for a period of over eight months. An illuminance meter was also mounted in the classroom to check the accuracy and stability of HDR images, and related illuminance values; these were found to agree with direct measurements, exhibiting a MBE of +20 lx (+10%) and a rRMSE of ±33 lx (±16%). The dataset did not exhibit any increase in typical errors (i.e., time drift) during the monitoring period.

When assessing statistical errors against HDR-derived illuminances, the 4CM showed better accuracy than the 2PH, especially when simulating illuminance for the wall region which received direct sunlight. In that case, the 4CM exhibited a rMBE = +4% and a rMAE = ±18%, whereas the 2PH exhibited a rMBE = +19% and a rMAE = ±25%. For other regions, situated towards the back of the room, the performance of the two methods was found to be largely similar, with rMBEs ranging from +17% to +34% and rMAEs of ±27–37%. The coefficients of determination calculated for the two methods and the four wall regions were found to be very similar too (r^2 = 0.79–0.84).

Last, long-term illuminance results were expressed as CBDM metrics, namely cumulative illumination (in *klxhr*) and UDI (with thresholds 100, 300, and 3000 lx), and such metrics were used to compare long-term performance as obtained from simulation and from HDR images. The analysis confirmed the tendency of simulation results to over-predict measurements by 5–34%, as noticed in the previous analyses. This could be explained by the lack of furniture and other details in the virtual model that might block light redistribution inside the space, otherwise correctly captured by results derived from HDR images.

Overall, the errors found in this study (±37%) are only marginally larger than those found in laboratory studies (±20%). As the space was not under controlled conditions, it is more difficult to determine exactly where the source of the errors is. Future studies should look at identifying and separating the effects of sky models, surface optical properties and occupant behaviour within the analysis of long-term daylight performance in occupied spaces. The method shows potential to be further applied in studies on visual comfort in existing buildings and on occupant behaviour modelling.

Funding

The research described in this paper was part of Dr Brembilla's PhD 'Applicability of Climate-Based Daylight Modelling' and Dr Drosou's PhD 'A framework to characterise operational daylighting performance in classrooms: measurement, observation and user perspectives'. Dr Brembilla's PhD was funded by the Engineering and Physical Sciences Research Council and by Arup Lighting UKMEA Group, under the EPSRC CASE Award scheme (Grant EP/K504476/1). Dr Drosou's PhD was funded by the UK Engineering and Physical Sciences Research Council through the London-Loughborough (LoLo) EPSRC Centre for Doctoral Training in Energy Demand (Grant EP/H009612/1).

CRediT authorship contribution statement

E. Brembilla: Writing – original draft, Conceptualization, Formal analysis, Visualization. **N.C. Drosou:** Investigation, Data curation, Conceptualization. **J. Mardaljevic:** Writing – review & editing, Supervision, Software, Investigation, Conceptualization.

Declaration of Competing Interest

The authors declare that they have no known competing financial interests or personal relationships that could have appeared to influence the work reported in this paper.

Acknowledgment

The authors welcome the helpful suggestions made the reviewers. Dr Drosou would like to thank the case study school's Head, Registrar, maintenance staff and students for enabling classroom access and participating in a year long monitoring study.

Appendix A

Relative errors were calculated with the following formulas [26]:

$$\mathrm{rMBE}\,[\%] = \frac{100}{\bar{x}} \sum_{i=1}^{N} y_i - x_i \tag{2}$$

$$\mathrm{rMAE}\,[\%] = \frac{100}{\bar{x}} \sum_{i=1}^{N} |y_i - x_i| \tag{3}$$

$$\mathrm{rRMSE}\,[\%] = \frac{100}{\bar{x}} \sqrt{\frac{\sum_{i=1}^{N} (y_i - x_i)^2}{N}} \tag{4}$$

where x is the observed value and y the predicted value. The term $\bar{x}$ indicates the mean of all observed values and the term N indicates the size of the population.

References

[1] Anna Carolina Menezes, et al., Predicted vs. actual energy performance of non-domestic buildings: Using post-occupancy evaluation data to reduce the performance gap, Appl. Energy 97 (2012) 355–364. issn: 03062619. doi: 10.1016/j.apenergy.2011.11.075..
[2] Paula van den Brom, Arjen Meijer, Henk Visscher, Performance gaps in energy consumption: household groups and building characteristics, Build. Res. Inf. 46 (1) (2018) 54–70, https://doi.org/10.1080/09613218.2017.1312897.
[3] Patrick X.W. Zou et al., Review of 10 years research on building energy performance gap: Life-cycle and stakeholder perspectives, Energy Build. 178 (2018) 165–181, https://doi.org/10.1016/j.enbuild.2018.08.040, issn: 14664321.
[4] Nishesh Jain et al., Cross-sectoral assessment of the performance gap using calibrated building energy performance simulation, Energy Build. 224 (2020) 110271, https://doi.org/10.1016/j.enbuild.2020.110271, issn: 03787788.
[5] Bill Bordass et al., Assessing building performance in use 3: energy performance of the Probe buildings, Build. Res. Inf. 29 (2) (2001) 114–128, https://doi.org/10.1080/09613210010008036, issn: 0961-3218.
[6] John Mardaljevic, Daylight Simulation: Validation, Sky Models and Daylight Coefficients (Ph.D. thesis), De Montfort University, Leicester, UK, 2000..
[7] C.F. Reinhart, Daylight availability and manual lighting control in office buildings: Simulation studies and analysis of measurement (Ph.D. thesis), University of Karlsruhe, Germany, 2001..
[8] Eleanor S. Lee, David Geisler-Moroder, Gregory Ward, Modeling the direct sun component in buildings using matrix algebraic approaches: Methods and validation, Solar Energy 160 (September 2017) (2018) 380–395, https://doi.org/10.1016/j.solener.2017.12.029, issn: 0038092X.
[9] Taoning Wang, Gregory Ward, Eleanor S. Lee, Efficient modeling of optically-complex, noncoplanar exterior shading: Validation of matrix algebraic methods, Energy Build. 174 (2018) 464–483, https://doi.org/10.1016/j.enbuild.2018.06.022, issn: 03787788.
[10] J. Alstan Jakubiec, Christoph F. Reinhart, A Concept for Predicting Occupants' Long-Term Visual Comfort within Daylit Spaces, Leukos 2724 (2015) 1–18, https://doi.org/10.1080/15502724.2015.1090880, issn: 1550-2724.
[11] J.A. Jakubiec, G. Quek, T. Srisamranrungruang, Long-term visual quality evaluations correlate with climate-based daylighting metrics in tropical offices – A field study, Lighting Res. Technol. (2020), https://doi.org/10.1177/1477153520926528, issn: 1477-1535..
[12] Geraldine Quek, J. Alstan Jakubiec, Calibration and Validation of Climate-Based Daylighting Models Based on One-Time Field Measurements: Office Buildings in the Tropics, LEUKOS 00.00 (2019), pp. 1–16. issn: 1550-2724. doi: 10.1080/15502724.2019.1570852..
[13] L. Doulos, A. Tsangrassoulis, F.V. Topalis, Multi-criteria decision analysis to select the optimum position and proper field of view of a photosensor, Energy Convers. Manage. 86 (2014) 1069–1077, https://doi.org/10.1016/j.enconman.2014.06.032, issn: 01968904..
[14] Laura Bellia, Francesca Fragliasso, Evaluating performance of daylight-linked building controls during preliminary design, Autom. Constr. 93 (2018) 293–314. issn: 09265805. doi: 10.1016/j.autcon.2018.05.026..
[15] Axel Jacobs, Getting the measure of daylight, Lighting J. (2014) 15–17..
[16] John Mardaljevic, Climate-Based Daylight Modelling And Its Discontents, in: CIBSE Technical Symposium. April. London, 2015, pp. 1–12..
[17] Nafsika Drosou, Eleonora Brembilla, John Mardaljevic, Reality bites : measuring actual daylighting performance in classrooms, in: PLEA 2016 Los Angeles - 36th International Conference on Passive and Low Energy Architecture, 2016, pp. 1–8.
[18] Greg Ward Larson, et al., Rendering with Radiance: the art and science of lighting visualization. San Francisco, CA, USA: Morgan Kaufmann Publishers Inc., 1998. isbn: 1-55860-499-5..
[19] R. Perez, R. Seals, J. Michalsky, All-weather model for sky luminance distribution-Preliminary configuration and validation, Solar Energy 50 (3) (1993) 235–245, https://doi.org/10.1016/0038-092X(93)90017-I, issn: 0038092X.
[20] J. Badosa, et al., Solar irradiances measured using SPN1 radiometers: uncertainties and clues for development, Atmospheric Meas. Tech. 7(12) (2014) 4267–4283. issn: 1867-8548. doi: 10.5194/amt-7-4267-2014..
[21] J. Mardaljevic et al., Reconstruction of cumulative daylight illumination fields from high dynamic range imaging: Theory, deployment and in-situ validation, Lighting Res. Technol. (2020) 1–21, https://doi.org/10.1177/1477153520945755, issn: 14771535.
[22] Eleonora Brembilla, C.J. Hopfe, John Mardaljevic, Influence of input reflectance values on climate-based daylight metrics using sensitivity analysis, J. Build. Performance Simul. 11(3) (2018) 333–349. issn: 1940-1493. doi: 10.1080/19401493.2017.1364786..
[23] Christian Humann, Andrew McNeil, Using HDR Sky Luminance Maps to Improve Accuracy of Virtual Work Plane Illuminance Sensors, Build. Simul. (2017) 1740–1748..
[24] Thijs Kruisselbrink, Rajendra Dangol, Evert van Loenen, Ceiling-Based Luminance Measurements: A Feasible Solution?, in: PROCEEDINGS OF the 29th Quadrennial Session of the CIE. Washington DC, USA: International Commission on Illumination, CIE, 2019, pp. 1166–1174. isbn: 978-3-902842-74-9. doi: 10.25039/x46.2019.PO077..
[25] Yujie Wu, Jérôme Henri Kämpf, Jean-Louis Scartezzini, Daylighting simulation for external Venetian blinds based on HDR sky luminance monitoring with matrix algebraic approach, Energy Proc. 158 (2019) 2677–2682. issn: 18766102. doi: 10.1016/j.egypro.2019.02.021..
[26] Christian A. Gueymard, A review of validation methodologies and statistical performance indicators for modeled solar radiation data: Towards a better bankability of solar projects, Renew. Sustain. Energy Rev. 39 (2014) 1024–1034, https://doi.org/10.1016/j.rser.2014.07.117, issn: 13640321.